Photoinduced processes in lead iodide perovskite solid-state solar cells

Arianna Marchioro[*a,b], Jan C. Brauer [a, c], Joël Teuscher [b], Michael Grätzel [b], and Jacques-E. Moser [a]

[a] Photochemical Dynamics Group; [b] Laboratory for Photonics & Interfaces, Institute of Chemical Sciences and Engineering; [c] Present adress : Laboratory for Macromolecular Organic Materials ; École Polytechnique Fédérale de Lausanne, 1015 Lausanne, Switzerland

ABSTRACT

Organic-inorganic hybrid systems based on lead halide compounds have recently encountered considerable success as light absorbers in solid-state solar cells. Herein we show how fundamental mechanistic processes in mesoporous oxide films impregnated with $CH_3NH_3PbI_3$ can be investigated by time resolved techniques. In particular, charge separation reactions such as electron injection into the titanium dioxide film and hole injection into the hole transporting material *spiro*-OMeTAD as well as the corresponding charge recombination reactions were scrutinized. Femtosecond transient absorption spectroscopy and time-resolved terahertz spectroscopy were applied to $CH_3NH_3PbI_3$ deposited either on TiO_2 or Al_2O_3 mesoporous films and infiltrated with the hole transporting material *spiro*-OMeTAD.

Keywords: lead iodide perovskite; *spiro*-OMeTAD; femtosecond transient absorption spectroscopy; terahertz spectroscopy; electron injection; hole injection.

1. INTRODUCTION

Recently, a new type of solid-state mesoscopic heterojunction solar cell has been reported, employing lead halide perovskite as the light absorbing material. This system, when deposited onto mesoporous TiO_2, was shown to provide remarkable photovoltaic power conversion efficiencies, up to 15%, in conjunction with the well-known *spiro*-OMeTAD acting as the hole transport material (HTM).[1] Remarkably, Lee et al. found that replacement of the mesoporous n-type TiO_2 with insulating Al_2O_3 could provide excellent power conversion efficiency, up to 10.9%.[2] Due to its large bandgap, electron injection from the perovskite to the aluminum oxide is not energetically allowed, and the Al_2O_3 purely acts like a mesoporous scaffold for the perovskite | *spiro*-OMeTAD system. The mechanistic processes in the device using mesoporous TiO_2 are still under debate, as these hybrid organic inorganic lead halide perovskite cumulate both functions of light absorption and n-type or p-type[3] conduction. The current mechanistic picture could be described as follows: The perovskite absorbs light and an excited state (electron-hole pair) is created. Charge separation can occur through two possible reactions: injection of a photogenerated electron into a TiO_2 nanoparticle (Eq. 1) or hole injection (Eq. 2) into a hole transporting material (HTM) such as *spiro*-OMeTAD or another organic hole transporter. While photo-induced absorption measurements in mixed halide systems ($CH_3NH_3Cl_2I$) have evidenced the electron injection process,[2] so far the same mechanistic pathway in $CH_3NH_3PbI_3$ system has been poorly studied. Charge separation reaction are in kinetic competition with other reactions such as exciton annihilation leading to photoluminescence (Eq. 3), non-radiative recombination (Eq. 4), as well as recombination of the charge carriers at the different interfaces (Eqs. 5, 6, 7).

Electron injection:

$$e^-_{perovskite} + TiO_2 \rightarrow e^-_{TiO_2} \quad (1)$$

Hole injection:

$$h^+_{perovskite} + HTM \rightarrow HTM^+ \quad (2)$$

* arianna.marchioro@epfl.ch

Physical Chemistry of Interfaces and Nanomaterials XII, edited by Natalie Banerji, Carlos Silva,
Proc. of SPIE Vol. 8811, 881108 · © 2013 SPIE · CCC code: 0277-786X/13/$18 · doi: 10.1117/12.2023003

Luminescence:

$$e^-_{perovskite} + h^+_{perovskite} \rightarrow hv \quad (3)$$

Non-radiative recombination:

$$e^-_{perovskite} + h^+_{perovskite} \rightarrow \nabla \quad (4)$$

Recombination of:

$$e^-_{TiO_2} + h^+_{perovskite} \rightarrow \nabla \quad (5)$$

$$e^-_{perovskite} + HTM^+ \rightarrow \nabla \quad (6)$$

$$e^-_{TiO_2} + HTM^+ \rightarrow \nabla. \quad (7)$$

Herein we report an optical spectroscopy study of solid-state methyl ammonium lead iodide ($CH_3NH_3PbI_3$) based films. Femtosecond transient absorption spectroscopy (TAS) has been applied to scrutinize mainly the processes of charge separation following light absorption in the device, on samples containing $CH_3NH_3PbI_3$ deposited either on TiO_2 or on Al_2O_3, and successively infiltrated with HTM. Time-resolved terahertz (THz) spectroscopy was also used to support these findings.

2. RESULTS AND DISCUSSION

2.1 Femtosecond transient absorption

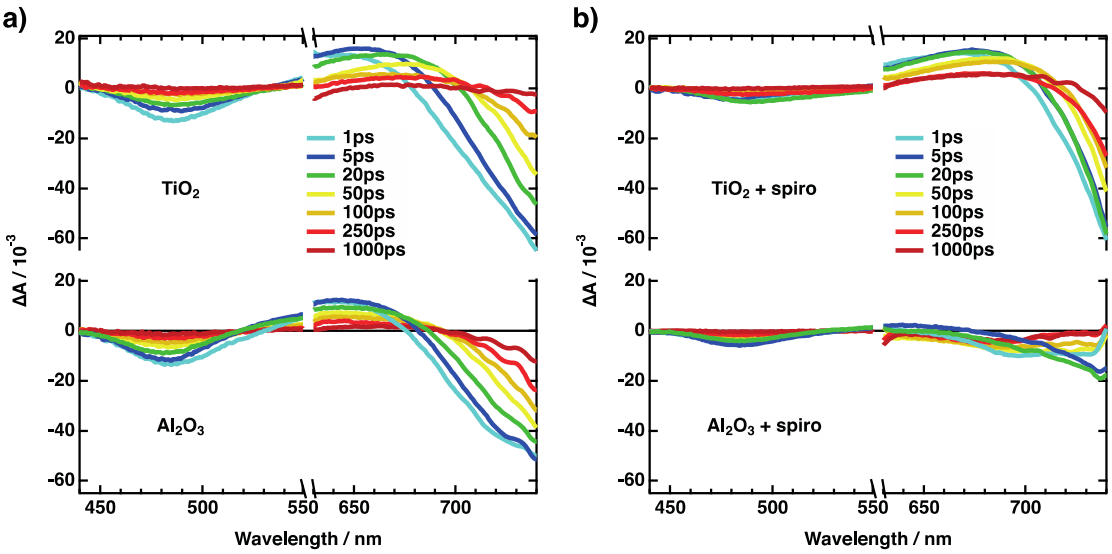

Figure 1: Femtosecond transient absorbance spectra with white light continuum probe and pulsed fs laser excitation at 580 nm of a) $CH_3NH_3PbI_3$ | TiO_2 and $CH_3NH_3PbI_3$ | Al_2O_3, b) *spiro*-OMeTAD | $CH_3NH_3PbI_3$ | TiO_2, and *spiro*-OMeTAD | $CH_3NH_3PbI_3$ | Al_2O_3, recorded at various time delays after excitation (color lines). Bleaching of the perovskite is evident with maximum at 480 nm, while the positive absorption signal in the 630 - 700 nm region corresponds to the excited state absorption. Negative feature in the red part of the spectra is attributed to stimulated emission. All transient features are decreased upon addition of the HTM. Adapted from ref. [6].

Femtosecond transient sbsorption studies have been performed in order to elucidate the mechanism of charge separation in the device. Four different samples, $CH_3NH_3PbI_3$ | TiO_2, with and without *spiro*-OMeTAD as well as $CH_3NH_3PbI_3$ | Al_2O_3, with and without *spiro*-OMeTAD, have been measured with 580 nm pulsed fs laser excitation and white light continuum (WLC) probe from 440 to 740 nm. Fig. 1a shows the samples deprived from HTM. Similar spectral features

can be observed : negative signal peaking at 483 nm is attributed to the bleaching of the ground state species of the perovskite, while the positive absorption signal in the 630 - 700 nm region is ascribed to the excited state absorption. Furthermore, the negative peak starting after 700 nm on both samples could be attributed to stimulated emission and matched the results obtained by steady-state emission.[4] Interestingly, global analysis of the observed dynamics (data not shown) evidence that a red-shift of both positive and negative bands in the 630-700 nm region is occurring on the ns timescale, indicating an electronic relaxation of the perovskite from an initial excited state.

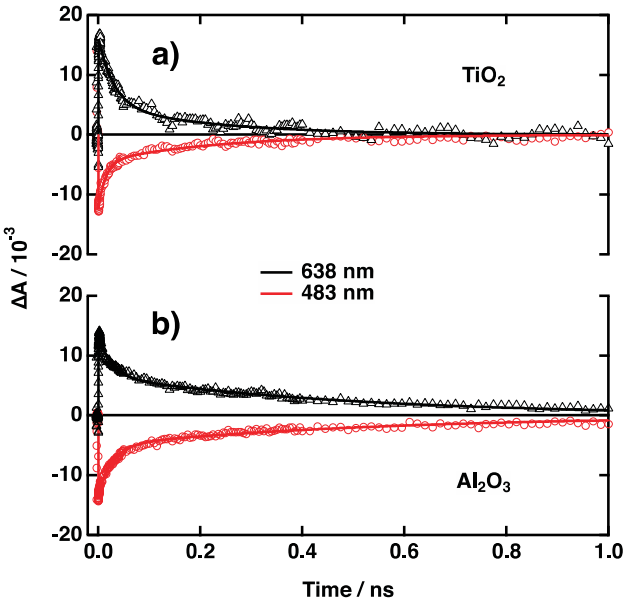

Figure 2 : Dynamics extracted at 483 nm (red circles) and 638 nm (black triangles) for a) $CH_3NH_3PbI_3$ | TiO_2 and b) $CH_3NH_3PbI_3$ | Al_2O_3. The solid lines represent convolution of one gaussian and two exponentials.

Furthermore, when the dynamics for positive signal and the bleaching (638 and 483 nm) are compared, they appear to be similar, confirming that the two species are related. The time constant for the first exponential (as obtained from a convolution of one gaussian and two exponentials) are respectively, for 638 and 483 nm : $CH_3NH_3PbI_3$ | TiO_2 : $\tau_{1(638)}$ = 30ps and $\tau_{1(483)}$ = 15ps while for $CH_3NH_3PbI_3$ | Al_2O_3 : $\tau_{1(638)}$ = 25ps and $\tau_{1(483)}$ = 27ps. The small differences observed between TiO_2 and Al_2O_3 are not significative enough to draw any conclusion regarding the electron injection process ; the recovery of the initial state in 1ns for both samples shows that no electron injection can be evidenced on these samples, thus matching very well the observed stimulated emission, fingerprint of an excited state over 1 ns.

Samples with hole conductor give another interesting insight on the working mechanisms of the perovskite-based cell (Fig. 1a). WLC spectrum of *spiro*-OMeTAD | $CH_3NH_3PbI_3$ | TiO_2 shows the same spectral features of the one without *spiro*-OMeTAD, with the bleaching peak in the blue region being less pronounced than in the case of $CH_3NH_3PbI_3$ | TiO_2 sample. Moreover, the stimulated emission peak appears to be less pronounced than in the aforementionned case, suggesting that a quenching of the fluorescence is occurring. In the case of of *spiro*-OMeTAD | $CH_3NH_3PbI_3$ | Al_2O_3, the amplitude of the 483 nm bleaching was found to be smaller than on a sample without hole conductor, as discussed previously for the *spiro*-OMeTAD | $CH_3NH_3PbI_3$ | TiO_2 sample. More interestingly, the positive peak in the 630-700 nm region completely disappeared, concomittantly with a net decrease of the stimulated emission negative peak. The results indicates a rapid quenching of the excited state by the *spiro*-OMeTAD through hole injection (Eq. 2), occurring in less than 1 ps. The difference in the amplitude of the quenching observed between TiO_2 and Al_2O_3 films might be related to the morphology, as for these experiments, the porosity of the films used was not the same and a difference in homogeneity of the films could be noticed (perovskite film deposited on Al_2O_3 being always more homogeneous). This difference in morphology is likely to be linked to a better pore filling by *spiro*-OMeTAD in the case of Al_2O_3, explaining thus why the reductive quenching by *spiro*-OMeTAD seems to be more efficient in this case. Further studies showed that

the amount of quenching is highly variable, and indeed, samples prepared according to the same experimental conditions as above were found to have the inverse behavior, i.e. quenching was more efficient on a TiO_2 sample (data not shown). This indicates that a fundamental parameter governing the contact between the perovskite and the HTM is not yet fully understood, at least while using the spin-coating deposition method for the perovskite.

2.2 THz spectroscopy

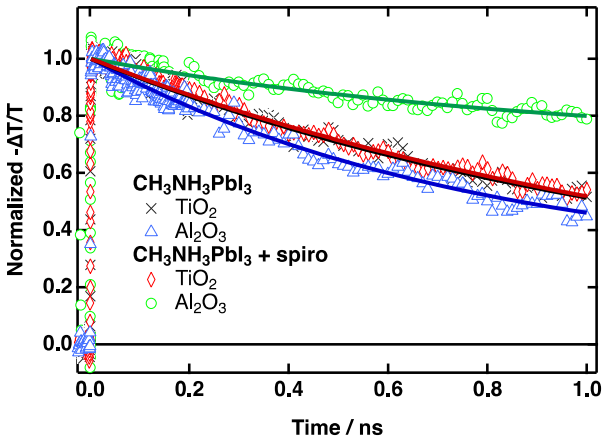

Figure 3: Terahertz transient signal following fs laser pulsed excitation at 580 nm. Signals reflect the time-evolution of the photoconductivity in the active layer. Black crosses: $CH_3NH_3PbI_3$ on TiO_2; blue triangles: $CH_3NH_3PbI_3$ on Al_2O_3; red diamonds: $CH_3NH_3PbI_3$ and spiro-OMeTAD on TiO_2; green circles: $CH_3NH_3PbI_3$ and spiro-OMeTAD on Al_2O_3. Thick lines are shown as guide to the eye.

Preliminary THz experiments are shown to support results found by TAS. THz probes the photoconductivity of the samples, i.e. the product of the mobility and the concentration of charge carriers. The photoconductivity in the active layer arises mainly from the charges in the perovskite material. Indeed, the observed signal is orders of magnitude higher than the one observed on bare TiO_2. Fig. 3 shows normalized transient THz signal for TiO_2 and Al_2O_3 mesoporous films, with and without the hole transporting material *spiro*-OMeTAD. Thus, following pulsed laser excitation at 580 nm, decay of THz signal reflects the time-evolution of the product of the mobilities and the population of mobile charge carriers. Decays were acquired over 1 ns and were qualitatively compared, thick lines are shown as a guide to the eye. Normalized dynamics for TiO_2 with and without HTM as well as Al_2O_3 sample without HTM were found to be in the same range, indicating that no significant difference attributed to charge separation either through electron or hole injection (Eqs. 1 and 2) can be evidenced. Interestingly, for the Al_2O_3 sample impregnated with HTM, the dynamics appears to be slower, thus suggesting that charge separation through hole injection (Eq. 2) is happening. This result matches what is observed in transient absorption data reported above, as the efficiency of the quenching by *spiro*-OMeTAD is more efficient in the case of the Al_2O_3 sample impregnated with HTM. In the case of THz signal, no conclusion can be drawn with regard to TiO_2 samples, however this might be related to the sensitivity of the measurement itself.

While revealing the hole injection pathway (Eq. 2), these studies do not allow to evidence the pathway of electron injection (Eq. 1). In a recent work by the author,[5] using ultrafast spectroscopy in the near infrared, transient absorbance of the charges in the perovskite was monitored. Results show that charge concentration decay is delayed upon infiltration of the hole transporting material *spiro*-OMeTAD, which is consistent with evidences of hole injection presented here above. Besides this particular charge separation pathway, evidence for electron injection from $CH_3NH_3PbI_3$ to the TiO_2 film is observed and appeared to lie in a similar timescale as the hole injection process. Confirmation of charge separation occurring through electron and hole injection is found in the microsecond timescale, using flash photolysis technique. Indeed, the oxidized *spiro*-OMeTAD transient concentration in the near infrared was monitored and revealed lifetimes for the recombination between either oxidized *spiro*-OMeTAD and $CH_3NH_3PbI_3$ (Eq. 6) or *spiro*-OMeTAD$^+$

and an e^-_{cb} (Eq. 7) of 15 µs and 99 µs, respectively. The longer lifetime observed for TiO_2 samples confirms the advantage of separating the charges through means of two interfaces, allowing for a more stable charge separation.

3. CONCLUSION

In conclusion, we show herein how fundamental processes in perovskite cells can be investigated by means of ultrafast spectroscopic techniques. Femtosecond transient absorption spectroscopy applied to $CH_3NH_3PbI_3$ films on TiO_2 and Al_2O_3 photoanodes reveals characteristic spectral features of this material, with the presence of a bleaching in the blue region, an excited state absorption in the 550-650 nm range and a large stimulated emission in the 700 nm region that is associated with the steady-state luminescence at 780 nm. Theses characteristic spectral features were not sufficient to unambiguously evidence electron injection through comparison between TiO_2 and Al_2O_3 photoanodes. However, quenching of the luminescence for samples impregnated with HTM could be correlated with the efficiency of the charge separation, and revealed that hole injection process (Eq. 2) is happening on a very short timescale (< 1ps). The apparent weaker quenching of the to $CH_3NH_3PbI_3$ excited state by the HTM in the TiO_2 sample compared to the Al_2O_3-based layer might be rationalized by a different morphology obtained on the different oxides mesoporous films. In Al_2O_3 films, a better pore filling by the *spiro*-OMeTAD could offer a better contact between the perovskite and the HTM and consequently yield a stronger reductive quenching of the photoexcited state. Time-resolved THz spectroscopy data, that observes transient photoconductivity corresponding to free charges and excitonic charges, support this hypothesis. Transient decay of mobile charges is observed on all perovskite samples, either on TiO_2 or Al_2O_3 framework. No major difference in the two layers is noticeable for samples that were not impregnated with HTM, as already observed in the visible transient absorption measurements. In the case of the HTM infiltrated samples, charge decay appears to be markedly slower only on an Al_2O_3 sample. This reveals that mobile charges are separated mainly at the *spiro*-OMeTAD interface, while the remaining charges thus recombine more slowly. The difference in the observed dynamics for TiO_2 and Al_2O_3 samples is thus mainly attributed to inhomogeneity of prepared samples and the discussion of the influence of the morphology on the observed spectroscopic signals will be the object of a separate study, where pathways of electron injection and hole injection appear to be closely related to the preparation of the perovskite layer.

4. METHODS

4.1 Sample preparation

Photoanode preparation for the transient absorption experiments has been reported elsewhere.[6] Sample preparation for THz experiments consisted in the following steps : 10 nm TiO_2 layer was deposited on microscopic quartz glasses by ALD to ensure adhesion of the mesoporous oxide films on quartz. TiO_2 and Al_2O_3 pastes were home made. For both oxides, a few drops of the paste were deposited on the ALD-treated quartz and spin-coated at 2000 rpm for 20 s. The TiO_2 film had an average thickness of ca. 500 nm. The procedure was repeated twice for Al_2O_3 and yielded films of ca. 200 nm. The films were then dried at 125°C for 5 min and subsequently sintered at 500°C for 30 min. To prepare $CH_3NH_3PbI_3$, CH_3NH_3I (0.1975 g, synthesized accordinf to the procedure already reported[6]) and PbI_2 (0.5785 g, 99% Aldrich) were mixed in 1 ml γ-butyrolactone at 60° C for overnight with stirring. The composition of the hole transport material solution was as follows : 218 mg of *spiro*-OMeTAD (Merck) was dissolved in 1 ml chlorobenzene (99,8%, Aldrich). 30.4 µλ of 4-tert butylpyridine were added as well as 100 µl of a previously prepared bis(trifluoromethane)sulfonimide lithium salt solution (LiTFSI, 99.95%, Aldrich) in acetonitrile (99.8%, Aldrich). 35 µl of he perovskite solution was spin-coated on the substrates (20 s. infiltration time, 2000 rpm for 30 s). Substrates were then dried for 15 min at 100°C. Samples containing hole transport material were prepared by spin-coating 30 µl of the *spiro*-OMeTAD solution (15 s. infiltration time, 4000 rpm for 30 s).

4.2 Femtosecond transient absorption

Transient absorption (TA) spectra were recorded using femtosecond pulsed laser pump-probe spectroscopy. The pump beam (580 nm) was generated with a commercial two-stage non-collinear optical parametric amplifier (NOPA-Clark,

MXR) from the 778 nm output of a Ti:sapphire laser system with a regenerative amplifier providing 150 fs pulses at a repetition rate of 1 kHz. The pump energy at the sample was at 200 nJ with a spot size diameter of 1 mm. The probe consisted of a white light continuum (430-1000 nm), generated by passing a portion of the 778 nm amplified Ti:sapphire output through a 3 mm thick sapphire plate. The probe intensity was always less than the pump intensity and the spot size was much smaller. The probe pulses were time delayed with respect to the pump pulses using a computerized translation stage. The probe beam was split before the sample into a signal beam (transmitted through the sample and crossed with the pump beam) and a reference beam. The signal and reference were detected with a pair of 163 mm spectrographs (Andor Technology, SR163) equipped with a 512x58 pixels back-thinned CCD (Hamamatsu S07030-0906) and assembled by Entwicklungsbüro Stresing, Berlin. To improve sensitivity, the pump light was chopped at half the amplifier frequency, and the transmitted signal intensity was recorded shot by shot. It was corrected for intensity fluctuations using the reference beam. The transient spectra were averaged until the desired signal-to-noise ratio was achieved (typically 3000 times). The polarization of the probe pulses was at magic angle relative to that of the pump pulses. All spectra were corrected for the chirp of the white-light probe pulses.

4. 3 Optical-pump THz-probe measurements

Optical-pump THz-probe spectroscopy is a purely optical technique to measure charge dynamics on an ultrafast time scale. The experimental setup can briefly be described as follows. The initial pulsed laser beam (1 kHz repetition rate, 45 fs pulse duration, 4.5 mJ/ pulse energy, $\lambda = 800$ nm wavelength) provided by an amplified Ti:Sapphire laser (Coherent Libra USP HE) is split into different paths. Approximately 1.4 mJ/ pulse is used to pump an OPerA-Solo optical parametric amplifier (Coherent), which is used as an optical pump to photo-generate carriers in the sample. A second part of the beam with approximately 0.9 mJ/ pulse energy is used to generate single cycle THz pulses by optical rectification in a 1 mm-thick ZnTe crystal. The THz beam is focused by gold mirrors on the sample and used as a probe. The transmitted THz pulses are detected in the time-domain through free space electro-optic sampling. A third part of the initial laser beam is used as a gating beam and guided over a delay line onto a 0.5 mm-thick ZnTe detector crystal. By varying the time delays between the optical pump, the THz probe pulse and the gating, amplitude and phase changes of the THz single-cycle pulses can be recorded. Changes of the amplitude of the THz pulses upon photo-excitation were measured in this work on a time scale of up to 1 ns with sub-ps time resolution. The pump beam was set at 580 nm and the typical power at the sample was 0.5 mW for a pump diameter of 2.7 mm corresponding to a fluence of ca. 9 $\mu J/cm^2$.

ACKNOWLEDGEMENTS

Financial support of this work by the Swiss National Science Foundation (SNF) through grant No 200020_134856 and the NCCR-MUST program is gratefully acknowledged.

REFERENCES

[1] Burschka, J., Pellet, N., Moon, S.-J., Humphry-Baker, R., Gao, P., Nazeeruddin, M.K., and Grätzel, M., "Sequential deposition as a route to high-performance perovskite-sensitized solar cells.," Nature 499 (7458), 316–319 (2013).

[2] Lee, M.M., Teuscher, J., Miyasaka, T., Murakami, T.N., and Snaith, H.J., "Efficient hybrid solar cells based on meso-superstructured organometal halide perovskites," Science 338 (6107), 643–647 (2012).

[3] Etgar, L., Gao, P., Xue, Z., Peng, Q., Chandiran, A.K., Liu, B., Nazeeruddin, M.K., and Grätzel, M., "Mesoscopic $CH_3NH_3PbI_3/TiO_2$ heterojunction solar cells.," Journal of the American Chemical Society 134 (42), 17396–17399 (2012).

[4] Papavassiliou, G.C., Mousdis, G.A., Koutselas, I.B., and Papaioannou, G.J., "Excitonic bands in the photoconductivity spectra of some organic-inorganic hybrid compounds based on metal halide units," International Journal of Modern Physics B 15 (28), 3727–3731 (2001).

[5] Marchioro, A. et al., Submitted.

[6] Kim, H.-S., Lee, C.-R., Im, J.-H., Lee, K.-B., Moehl, T., Marchioro, A., Moon, S.-J., Humphry-Baker, R., Yum, J.-H., et al., "Lead Iodide Perovskite Sensitized All-Solid-State Submicron Thin Film Mesoscopic Solar Cell with Efficiency Exceeding 9%," Scientific Reports 2, (2012).